PHYSICAL REVIEW D **74,** 064025 (2006)

Collisions of rigidly rotating disks of dust in general relativity

Jörg Hennig* and Gernot Neugebauer

Theoretisch-Physikalisches Institut, Friedrich-Schiller-Universität Jena, Max-Wien-Platz 1, D-07743 Jena, Germany

(Received 7 June 2006; published 22 September 2006)

We discuss inelastic collisions of two rotating disks by using the conservation laws for baryonic mass and angular momentum. In particular, we formulate conditions for the formation of a new disk after the collision and calculate the total energy loss to obtain upper limits for the emitted gravitational energy.

DOI: 10.1103/PhysRevD.74.064025 PACS numbers: 04.20.Jb, 04.25.Nx, 04.30.Db, 95.30.Sf

I. INTRODUCTION

Disk-like matter configurations play an important role in astrophysics (e.g. as models for galaxies, accretion disks or intermediate phases in the merger process of two neutron stars). The simplest models for such configurations are disks of dust. From a mathematical point of view they are solutions to boundary value problems of the Einstein equations. Explicit solutions in terms of standard functions or integrals are known for *rigidly rotating disks of dust* [1–5] (the only known solutions for isolated rigidly rotating bodies) and *counterrotating disks of dust*, consisting of clockwise and counterclockwise rotating dust particles (see e.g. [6,7] or [8]).

In this paper we want to study inelastic collisions of rotating disks. (Because of the gravitational radiation there exist no *elastic* collisions in general relativity.) A rigorous mathematical description of such merging processes is extremely difficult, for the solution of the corresponding initial boundary value problem requires extensive numerical investigations. We adopt a different method and perform a ''thermodynamic'' analysis. In this way we forgo the detailed analysis in favor of a simpler description leading to a ''rough'' picture of the merging processes. A classical example for this procedure was given by Hawking and Ellis who discussed the efficiency of the collision and coalescence of two black holes, cf. [9]. By using the area theorem for black holes they obtained, for spherically symmetric black holes, an upper limit for the efficiency of conversion of mass into gravitational radiation of $1 - 1/\sqrt{2} \approx 29.3\%$. One of our results will be a similar limit for the coalescence of two disks as an example for ''normal matter'' collisions. Considerations like these are typical for thermodynamics, in which initial and final equilibrium states are linked by conserved quantities bridging the intermediate nonequilibrium states of the system. Interestingly, a Gibbs equation for the thermodynamical potential *energy (-mass)* M as a function of baryonic mass M_0 and angular momentum J can be formulated even in the case of rotating dust matter, see Eq. (15).

In particular, we study the ''head on'' collision of two aligned rigidly rotating disks of dust with parallel [scenario (a)] or antiparallel [scenario (b)] angular momenta, cf. Fig. 1. Rigid rotation is a universal limit for rotating disks of dust. Any amount of friction between the rings comprising the disk of dust will lead to an equilibrium state with constant angular velocity Ω after a sufficiently long time. As a consequence, *rigidly* rotating disks are characterized by an extremum in the binding energy, compared to *differentially* rotating disks with the same baryonic mass and angular momentum, see appendix A. We assume that the initial distance between the disks is large enough to keep the initial gravitational interaction very small.

As already mentioned, the dynamics of the collision process is outside the scope of our considerations. However, we know that the total baryonic mass M_0 and the total angular momentum J are conserved. Finally, due to the outgoing gravitational radiation and possible dissipative processes, the collision ends in a stationary (and axisymmetric) configuration with the total baryonic mass M_0 and the total angular momentum J.

In this paper we confine ourselves to two problems: the formation of a rigidly rotating disk (RR disk) from two rigidly rotating initial disks and, as a second example, the formation of the rigidly counterrotating disk described by Bardeen, and Morgan and Morgan [6] (RCR disk) from two rigidly rotating initial disks with opposite angular momenta. We will discuss questions like these: For which parameter values of the initial disks can the collision lead to a rigidly rotating or rigidly counterrotating disk at all? Which domain of the M_0-J-parameter space can be reached by such processes? As we will see in Sec. II A 2, the relative binding energy E_b of the rigidly counterrotating disks takes positive as well as negative values.

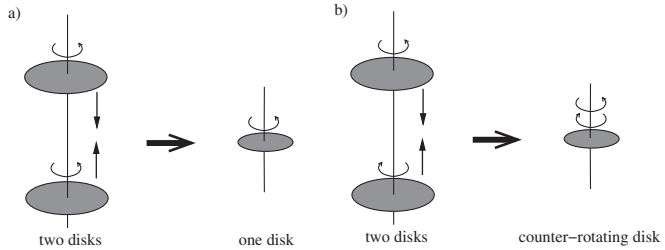

FIG. 1. Illustration of the two collision scenarios

*Electronic address: J.Hennig@tpi.uni-jena.de

Therefore, it is an interesting question if the formation of RCR disks with a negative binding energy is a possible result of collision processes. Finally, we calculate upper limits for the energy loss due to gravitational radiation in such collision processes.

The mathematical analysis of these problems requires the examination of the ''thermodynamics'' of *rigidly rotating disks* and *rigidly counterrotating disks* and the discussion of the equations of state for mass and angular momentum. This is done in Sec. II. In Sec. III we discuss limits for the formation of disks after the collision. The conservation equations can be used to calculate the parameters of the merged disks in terms of elliptic functions. This analysis and the resulting plots can be found in Sec. IV. The energy loss, i.e. the efficiency of the two scenarios is calculated in Sec. V.

The metric coefficients of the rigidly rotating disk of dust solution are given in terms of ultraelliptic theta functions which reduce to elliptic functions along the axis of symmetry. Since the multipole moments for energy (-mass) M and angular momentum J, as the central quantities of our thermodynamic considerations, can be read off from the axis values of the metric, our analysis has to make extensive use of elliptic functions. To avoid lengthy calculations in the main body of the text, we relegate the analytic expressions to the appendix and present the results in graphical form in the main text.

For the sake of simplicity, we restrict ourselves to identical initial disks (i.e. disks of equal baryonic mass and equal absolute values for the angular momenta). The generalization to different disks is a straightforward procedure.

II. "THERMODYNAMICS" OF DISK MODELS

A. Disk of dust solutions

1. Rigidly rotating disks of dust

This section is devoted to a thermodynamic description of the ''ingredients'' of the collision processes: rigidly rotating disks (RR disks) and rigidly counterrotating disks (RCR disks).

The free boundary value problem for the relativistic rigidly rotating disk of dust was approximately discussed by Bardeen and Wagoner [4,5] and analytically solved in terms of ultraelliptic theta functions by Neugebauer and Meinel [1–3] using the inverse scattering method. For a discussion of the physical properties see [10]. The solution is stationary (Killing vector: ξ^i) and axisymmetric (Killing vector: η^i). Its line element together with the Killing vectors can therefore be written in the Weyl-Lewis-Papapetrou standard form

$$ds^2 = e^{-2U}[e^{2k}(d\rho^2 + d\zeta^2) + \rho^2 d\varphi^2] - e^{2U}(dt + a d\varphi)^2,$$
$$\xi^i = \delta^i_t, \qquad \eta^i = \delta^i_\varphi, \tag{1}$$

where U, k and a are functions of ρ and ζ alone and δ^i_k is the four-dimensional Kronecker symbol. Note that we use the normalized units where $c = 1$ for the speed of light and $G = 1$ for Newton's gravitational constant. The solution can be written in terms of the complex Ernst potential $f(\rho, \zeta) = e^{2U(\rho,\zeta)} + ib(\rho, \zeta)$, where the imaginary part is related to a by $a_{,\rho} = \rho e^{-4U} b_{,\zeta}$ and $a_{,\zeta} = -\rho e^{-4U} b_{,\rho}$. In this formulation, the vacuum Einstein equations are equivalent to the Ernst equation

$$(\Re f)\left(f_{,\rho\rho} + f_{,\zeta\zeta} + \frac{1}{\rho} f_{,\rho}\right) = f^2_{,\rho} + f^2_{,\zeta}. \tag{2}$$

(k can be calculated via a path integral from the Ernst potential f.)

The matter of the disk of dust is described by the energy-momentum tensor

$$T^{ij} = \varepsilon u^i u^j, \qquad \varepsilon = \sigma(\rho)\delta(\zeta), \tag{3}$$

where ε, σ and u^i are the mass density, the surface mass density ($\sigma(\rho) = 0$ if $\rho > \rho_0$, ρ_0 being the coordinate radius of the disk) and the four-velocity of the dust particles, respectively. For rigidly rotating bodies, the four-velocity is a linear combination of the two killing vectors,

$$u^i = e^{-V_0}(\xi^i + \Omega \eta^i), \tag{4}$$

where Ω is the constant angular velocity of the body. Here, as a consequence of the geodesic motion of the dust particles, the coefficient e^{-V_0} turns out to be a constant too,

$$V_0 = \text{constant}. \tag{5}$$

The RR disk solution depends on two parameters. As an example, one may choose the coefficients e^{-V_0} and Ωe^{-V_0} of the linear combination (4) or, alternatively the coordinate radius ρ_0 of the disk and a centrifugal parameter $\mu = 2\Omega^2 \rho_0^2 e^{-2V_0}$ ($\mu \to 0$ turns out to be the Newtonian limit and $\mu \to 4.629\,66\ldots$ the ultrarelativistic limit, where the disk approaches the extreme Kerr black hole, cf. [2,10] for these and further properties).

The baryonic mass M_0, the gravitational (ADM) mass M and the angular momentum J of the disk are given by

$$M_0 = \int_\Sigma \varepsilon \sqrt{-g} u^t d^3x, \tag{6}$$

$$M = 2\int_\Sigma (T_{ij} - \tfrac{1}{2} T g_{ij}) n^i \xi^j dV, \tag{7}$$

$$J = -\int_\Sigma T_{ij} n^i \eta^j dV, \tag{8}$$

with T_{ij} as in (3). Σ is the spacelike hypersurface $t =$ constant with the unit future-pointing normal vector n^i.

2. Rigidly counterrotating disks of dust

An interesting example of a counterrotating disk is the RCR disk by Bardeen, Morgan and Morgan [6], consisting of a clockwise and a counterclockwise rotating component

of dust. All mass elements move along geodesic lines and the two components have constant angular velocities with opposite signs. Since the net angular momentum of the disk vanishes, its metric can be written in the *static* Weyl-Lewis-Papapetrou form [$a = 0$ in (1)],

$$\begin{aligned} ds^2 &= e^{-2U}[e^{2k}(d\rho^2 + d\zeta^2) + \rho^2 d\varphi^2] - e^{2U}dt^2, \\ \xi^i &= \delta^i_t, \qquad \eta^i = \delta^i_\varphi, \qquad \xi^i\eta_i = 0. \end{aligned} \tag{9}$$

The metric functions U and k are standard integrals, see appendix D. Here the energy-momentum tensor is the superposition of two expressions (3),

$$\begin{aligned} T^{ij} &= \tfrac{1}{2}\varepsilon(u^i u^j + v^i v^j), \qquad u^i = e^{-V_0}(\xi^i + \Omega\eta^i), \\ & v^i = e^{-V_0}(\xi^i - \Omega\eta^i), \end{aligned} \tag{10}$$

where u^i and v^i denote the four-velocities of the counterclockwise and clockwise moving dust particles. Just as for the case of the RR disk, V_0 turns out to be a constant as a consequence of the constant angular velocity Ω and the geodesic motion of the dust particles, and the solution is again governed by two parameters. As with the RR disks, these could be chosen to be the coordinate radius ρ_0 of the disk and the centrifugal parameter $\mu = 2\Omega^2\rho_0^2 e^{-2V_0}$. However, it turns out that, instead of μ, the parameter $b = \Omega\rho_0 e^{-2V_0}$ simplifies the discussions. ($b \to 0$ is the Newtonian limit and $b \to \infty$ the ultrarelativistic limit.)

The baryonic mass M_0 and the gravitational mass M of the RCR disk and the angular momenta $\pm J$ of the counterclockwise and clockwise rotating part (the resulting angular momentum vanishes) can again be calculated from the Eqs. (6)–(8) (where in the formula for J only the energy-momentum tensor of the counterclockwise rotating dust component is used). For the calculation we refer to appendix C.

B. Equilibrium and stability

Equilibrium configurations can be described with the aid of variational principles (cf. [11,12]). For disks of dust we may consider the thermodynamic potential

$$E := \int_{t=t_0}\left(\frac{R}{8\pi} + \varepsilon\right)\sqrt{-g}\,d^3x + n\Omega J + \frac{M}{2}, \tag{11}$$

where R is the Ricci scalar and n indicates the number of dust components ($n = 1$ for RR disks and $n = 2$ for RCR disks). The variation of E leads to

$$\begin{aligned} \delta E = &-\frac{1}{8\pi}\int\left(R^{ij} - \frac{R}{2}g^{ij} + 8\pi T^{ij}\right)\sqrt{-g}\,\delta g_{ij}\,d^3x \\ &+ e^{V_0}\delta M_0 + n\Omega\delta J, \end{aligned} \tag{12}$$

with T^{ij} from (3) or (10) and M_0, M and J from (6)–(8). Obviously, for fixed baryonic mass M_0 and fixed angular momentum J, i.e. $\delta M_0 = 0$ and $\delta J = 0$, the condition $\delta E|_{M_0,J} = 0$ leads to the Einsteinian field equations. On the other hand, for solutions to the field equations it turns out that E is equal to the gravitational mass M. Hence, one obtains

$$\delta M = e^{V_0}\delta M_0 + n\Omega\delta J. \tag{13}$$

To illustrate the meaning of the potential E we should mention that the Newtonian limit of Eq. (11) is given by

$$E = M_0 + \frac{1}{2}\int \rho^{\mathrm{N}} U^{\mathrm{N}} d^3x + n\frac{J^2}{2I}, \tag{14}$$

where ρ^{N}, U^{N} and I are the Newtonian mass density, the Newtonian gravitational potential and the moment of inertia of the disk, respectively. In this limit, E is the sum of the rest energy M_0c^2 ($c = 1$), the potential energy and the rotational energy. The function E in Eq. (14) is precisely the quantity that was used by Katz in [13] to study equilibrium and stability of Maclaurin and Jacobi ellipsoids in Newtonian theory. In subsection II C 2 we will use the relativistic generalization (11) of E to investigate the stability of counterrotating (RCR) disks of dust.

C. Applications

1. Rigidly rotating disks of dust

The extensive quantities M_0, M and J are not independent of each other. Because of Eq. (13) (with $n = 1$) they have to satisfy the Gibbs formula (see also [5,12] or [14])

$$dM = e^{V_0}dM_0 + \Omega dJ, \tag{15}$$

where $M = M(M_0, J)$ is a potential in M_0, J. Other potentials can be obtained via Legendre transformations. As an example we may use, as a consequence of (6)–(8), the parameter relation

$$M = e^{V_0}M_0 + 2\Omega J \tag{16}$$

to eliminate M in (15). We arrive at

$$d(\Omega J) = -Jd\Omega - e^{V_0}M_0 dV_0, \tag{17}$$

and can now use the potential ΩJ to calculate J and M as functions of the pair Ω and V_0 or, alternatively, Ω and μ. To get explicit expressions for these "equations of state" we make use of the disk of dust solution [1–3] to obtain

$$\Omega J = \frac{e^{V_0}}{4\Omega}\int_0^\mu e^{-V_0(x)}b_0'(x)dx - \frac{1}{4\Omega}b_0(\mu), \tag{18}$$

where b_0 is the imaginary part of the Ernst potential in the center of the disk, $b_0 = b(\rho = 0, \zeta = 0^+)$, and, as a consequence of (17),

$$\begin{aligned} M_0(\Omega, \mu) &= -e^{-V_0}\frac{\partial(\Omega J)}{\partial V_0}\bigg|_\Omega \\ &= -\frac{1}{4\Omega}\int_0^\mu e^{-V_0(x)}b_0'(x)dx, \end{aligned} \tag{19}$$

$$J(\Omega, \mu) = -\left.\frac{\partial(\Omega J)}{\partial \Omega}\right|_{V_0} = \frac{e^{V_0}}{4\Omega^2}\int_0^\mu e^{-V_0(x)} b_0'(x)\mathrm{d}x - \frac{1}{4\Omega^2} b_0(\mu). \quad (20)$$

The parameter relation (16) takes the form

$$M = e^{V_0} M_0 + 2\Omega J = -e^{V_0} M_0 - \frac{1}{2\Omega} b_0(\mu). \quad (21)$$

For explicit expressions for the metric coefficients $b_0(\mu)$, $V_0(\mu)$, the masses M_0 and M and the angular momentum J in terms of elliptic functions see appendix B.

There is an interesting scaling behavior of the disk parameters. For example $\Omega\rho_0$, ΩM, ΩM_0, $\Omega^2 J$, M/M_0, M^2/J and M_0^2/J depend only on the centrifugal parameter μ but not on a second parameter, cf. (19)–(21) and appendix B.

For an illustration of the equations of state Fig. 2 shows relations between ΩM_0, M_0^2/J and the relative binding energy $E_b = 1 - M/M_0$. The figure also displays the coordinate radius ρ_0 and the "circumferential radius" ρ_c (defined as $\rho_c = \frac{1}{2\pi}\int \mathrm{d}s|_{\rho=\rho_0, t=t_0, \zeta=0} = \sqrt{g_{\varphi\varphi}}|_{\rho=\rho_0, t=t_0, \zeta=0}$). Thereby $E_b \to 0$ and $E_b \to 0.3733\ldots$ are the Newtonian and the ultrarelativistic limit, respectively. The picture demonstrates the "parametric collapse" of a disk towards the black hole limit [15]: Consider a disk with a fixed number of baryons (i.e. fixed M_0) occupying states with decreasing energy M. Then, the angular velocity increases and the angular momentum decreases while the disk shrinks ($\rho_0 \to 0$, while the "true" radius remains strictly positive, $\rho_c \to 1.4372\ldots \cdot M_0$). In the limit $E_b = 0.3733\ldots$, $M_0^2/J = 2.5460\ldots$ one obtains a ratio $M^2/J = M_0^2/J \cdot (1 - E_b)^2 = 1$ corresponding to the extreme Kerr black hole [15].

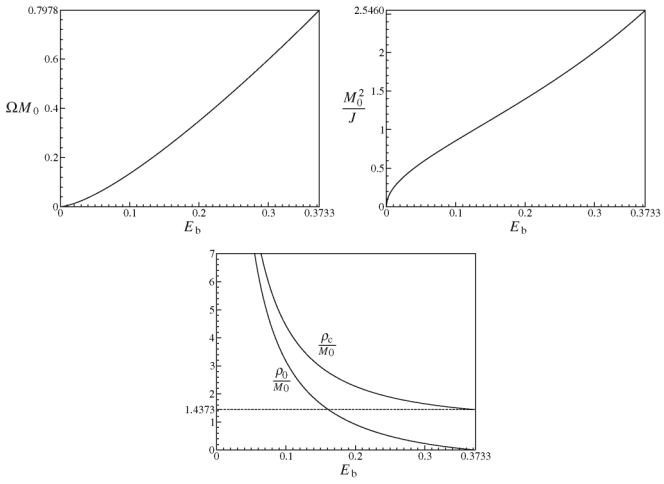

FIG. 2. ΩM_0, M_0^2/J and the radii ρ_0 and ρ_c as functions of the relative binding energy $E_b = 1 - M/M_0$ for the rigidly rotating disk of dust.

2. Rigidly counterrotating disks of dust

As in the case of RR disks we can formulate a Gibbs relation for RCR disks, too. From Eq. (13) (with $n = 2$) we obtain

$$\mathrm{d}M = e^{V_0}\mathrm{d}M_0 + 2\Omega\mathrm{d}J. \quad (22)$$

A Legendre transformation leads to the potential ΩJ satisfying the equation

$$\mathrm{d}(\Omega J) = -J\mathrm{d}\Omega - \tfrac{1}{2}e^{V_0} M_0 \mathrm{d}V_0. \quad (23)$$

From the analytic solution we find

$$\Omega J(\Omega, V_0) = \frac{1}{8\pi\Omega}\int_0^{\sqrt{e^{-4V_0}-1}} \left(\frac{1}{\sqrt{1+t^2}} - e^{2V_0}\right) \times \frac{t \arctan t}{1+t^2}\mathrm{d}t. \quad (24)$$

This potential can be used to calculate the baryonic mass M_0 and the angular momentum J via

$$M_0 = -2e^{-V_0}\left.\frac{\partial(\Omega J)}{\partial V_0}\right|_\Omega, \qquad J = -\left.\frac{\partial(\Omega J)}{\partial \Omega}\right|_{V_0}, \qquad M = e^{V_0} M_0 + 4\Omega J, \quad (25)$$

where V_0 and Ω are related to the parameters ρ_0 and b by the equations

$$e^{-4V_0} = 1 + 4b^2, \qquad \Omega\rho_0 = b/\sqrt{1+4b^2}. \quad (26)$$

The RCR disks show the same scaling behavior of the disk parameters as the RR disks, e.g. $\Omega\rho_0$, ΩM, ΩM_0, $\Omega^2 J$, M/M_0, M^2/J and M_0^2/J depend only on the parameter b and not on the coordinate radius ρ_0.

An interesting feature of the RCR disks is the strange behavior of the binding energy, which is negative for $b > 4.1074\ldots$ as shown in Fig. 3. Interestingly, there are several physical arguments against the formation of RCR disks in this region. In fact, the following application of the stability analysis of sec. II B will show a transition from stability to instability at $b = 1.3393\ldots$, even before the

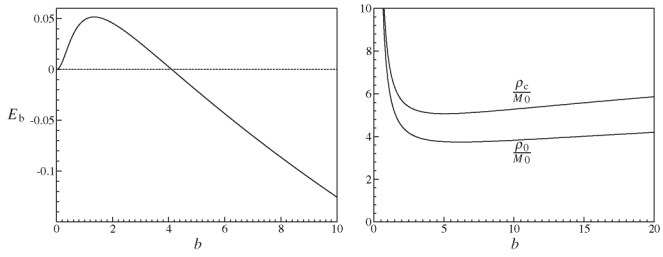

FIG. 3. Left picture: The relative binding energy $E_b = 1 - M/M_0$ of the RCR disk as a function of the centrifugal parameter b. E_b reaches negative values in the relativistic region (large b). Right picture: The coordinate radius ρ_0 and the "circumferential radius" ρ_c divided by the baryonic mass M_0 as functions of the centrifugal parameter b.

binding energy E_b becomes negative. Moreover, using a general argument resulting from the baryonic mass conservation we will show in the next section that RCR disks with negative binding energy cannot form by collision.

Figure 3 also shows ρ_0/M_0 and ρ_c/M_0 as functions of b (right picture), with ρ_c defined as in subsection II C 1. For increasing b the radii first decrease, reach a minimum and increase again. There is no "parametric collapse" of the RCR disks towards a black hole.

In order to understand the strange behavior of the binding energy we now apply the stability analysis of sec. II B to RCR disks. Calculating the Ricci scalar R of the metric (9) we obtain from (11)

$$E = \int\left[\frac{1}{8\pi}(\nabla U)^2 + \varepsilon\sqrt{-g}\right]\mathrm{d}\rho\mathrm{d}\varphi\mathrm{d}\zeta + 2\Omega J. \tag{27}$$

Note that the term $M/2$ in (11) is compensated by a surface term resulting from the integration over R. The variation $\delta E|_{M_0,J} = 0$ leads to the equations

$$\begin{aligned} \triangle U &= S(\rho)\delta(\zeta), \\ S(\rho)\delta(\zeta) &:= -\mathrm{e}^{2k-2U}(T^t_t - T^\varphi_\varphi) \\ &= \varepsilon\mathrm{e}^{2k-2V}(1+\Omega^2\rho^2\mathrm{e}^{-4U}), \end{aligned} \tag{28}$$

$$\begin{aligned} M_0 &= \int \varepsilon\mathrm{e}^{-V}\sqrt{-g}\mathrm{d}\rho\mathrm{d}\varphi\mathrm{d}\zeta = \text{ constant}, \\ J &= \int \frac{\varepsilon}{2}\mathrm{e}^{-V}\eta_i u^i\sqrt{-g}\mathrm{d}\rho\mathrm{d}\varphi\mathrm{d}\zeta = \text{ constant}. \end{aligned} \tag{29}$$

Using the relation (28) and the equation $\mathrm{e}^{2V} = \mathrm{e}^{2U}(1 - \Omega^2\rho^2\mathrm{e}^{-4U})$ as a consequence of $u^i u_i = v^i v_i = -1$, (27) can be rewritten as

$$E = 2\pi\int\left[-\frac{1}{2}SU + \frac{\mathrm{e}^{4U} - \Omega^2\rho^2}{\mathrm{e}^{4U} + \Omega^2\rho^2}S\right]\mathrm{d}\rho + 2\Omega J. \tag{30}$$

In the same way we calculate the baryonic mass M_0 and the angular momentum J as defined in (29),

$$M_0 = 2\pi\int_0^{\rho_0}\frac{\sqrt{\mathrm{e}^{4U} - \Omega^2\rho^2}}{\mathrm{e}^{4U} + \Omega^2\rho^2}S(\rho)\mathrm{e}^U\rho\mathrm{d}\rho, \tag{31}$$

$$J = \pi\Omega\int_0^{\rho_0}\frac{S(\rho)}{\mathrm{e}^{4U} + \Omega^2\rho^2}\rho^3\mathrm{d}\rho. \tag{32}$$

Now we consider the two-parametric family of functions

$$S(\rho;\rho_0,b) = \frac{b}{\pi^2\rho_0}\frac{1}{\sqrt{1+4b^2\frac{\rho^2}{\rho_0^2}}}\arctan\frac{2b\sqrt{1-\frac{\rho^2}{\rho_0^2}}}{\sqrt{1+4b^2\frac{\rho^2}{\rho_0^2}}} \tag{33}$$

and the corresponding disk potential [as a solution of (28)]

$$U(\rho;\rho_0,b) = \frac{1}{2}\ln\frac{1+\sqrt{1+4b^2\frac{\rho^2}{\rho_0^2}}}{2\sqrt{1+4b^2}}, \tag{34}$$

where b and ρ_0 are arbitrary constants. Obviously, E depends on the parameters b, ρ_0 and Ω, $E = E(b,\rho_0,\Omega)$. It should be emphasized that $S(\rho;\rho_0,b)$ and $U(\rho;\rho_0,b)$ define a family of trial functions which do *not* satisfy the Eq. (29). Only if b, ρ_0 and Ω are connected by the relation (26) we arrive at the RCR disk solution. To calculate the extremum of E for fixed values of M_0, J ($\delta E|_{M_0,J} = 0$) we replace ρ_0 and Ω via (31) and (32) by M_0 and J. With the explicit expressions (33) and (34), M_0, J and E take the form

$$\begin{aligned} M_0 &= \rho_0 g_1(b,\Omega\rho_0), \qquad J = \Omega\rho_0^3 g_2(b,\Omega\rho_0), \\ E &= \rho_0 g_3(b,\Omega\rho_0) + 2\Omega J \end{aligned} \tag{35}$$

with functions g_1, g_2 and g_3 expressible in terms of integrals resulting from (30)–(32). The combination

$$s := M_0^2/J = \frac{g_1(b,\Omega\rho_0)}{\Omega\rho_0 g_2(b,\Omega\rho_0)} \tag{36}$$

allows to express $\Omega\rho_0$ in terms of b and s, $\Omega\rho_0 = g_4(b;s)$. Hence, we finally obtain E in the form

$$\begin{aligned} E &= M_0\frac{g_3[b,g_4(b;s)] + 2g_4^2(b;s)g_2[b,g_4(b;s)]}{g_1[b,g_4(b;s)]} \\ &=: -M_0\tilde{E}(b;s), \end{aligned} \tag{37}$$

where the dependence of $\tilde{E}$ on b and s is given implicitly by some integral relations. The minima of E for fixed M_0 and J are the maxima of $\tilde{E}$ for fixed s and vice versa.

The numerical discussion of $\tilde{E}(b;s)$ leads to the following results: The extremum condition $\partial\tilde{E}/\partial b = 0$ yields the parameter relation (26). That means the RCR disk solution is an extremum of $\tilde{E}$ (at least a stationary point). As it was shown by Poincaré and discussed by Katz in [13], stability can be analyzed with the help of conjugate variables with respect to a thermodynamic potential. Here, we may choose the variable s and its conjugate $K(s)$ with respect to $\tilde{E}$,

$$K(s) := \frac{\partial\tilde{E}}{\partial s}[b_e(s),s], \tag{38}$$

where $b = b_e(s)$ is the equilibrium relation between b and s. Figure 4 shows the pair $[s,K(s)]$. The criterion for a change of stability is the existence of a vertical tangent to this curve. Obviously, such a behavior is given at the point A where $s = 0.9634\ldots$ ($b = 1.3393\ldots$). A careful numerical analysis of the curve $K(s)$ shows that there is no other point with a vertical tangent. Since a stable branch can be identified as the one with a positive slope near the vertical tangent, we conclude that the lower branch in Fig. 4 is stable according to Poincaré's definition and the upper branch (dashed curve) is unstable: *RCR disks are unstable for* $b > 1.3393\ldots$ This result includes the *instability of RCR disks with negative binding energy* E_b ($E_b < 0$ for $b > 4.1074\ldots$).

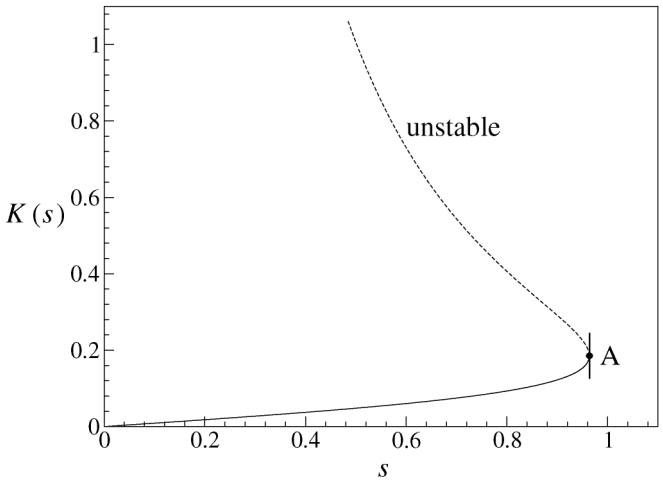

FIG. 4. The pair of conjugate variables s and $K(s)$ for the RCR disk. At the point A the parameter s takes the "critical" value $s = 0.9634\ldots$ (corresponding to $b = 1.3393\ldots$). The vertical tangent at that point indicates a change of stability.

Because of the definition (36), M_0^2/J takes its maximum just at the critical value $b = 1.3393\ldots$ (see Fig. 6).

III. PARTICULAR COLLISION PROCESSES

A. Conservation laws

As mentioned before, we consider "head on" collisions of rigidly rotating disks of dust for parallel and antiparallel angular momenta as sketched in Fig. 1 [from now on denoted as scenario (a) and scenario (b), respectively]. To compare the initial disks with the resulting merged disk we will make use of conservation laws. Obviously, there are two conserved quantities. One of them is the *baryonic mass*. Considering two colliding bodies A and B, we have

$$\tilde{M}_0 = M_0^A + M_0^B, \tag{39}$$

where the baryonic mass $\tilde{M}_0$ of the final body is the sum of the baryonic masses M_0^A and M_0^B of the colliding bodies (from now on, tildes denote quantities of the final bodies). A first consequence of (39) is that the (inelastic) collision of two bodies with positive binding energies cannot lead to a body with a negative binding energy. Namely,

$$\tilde{M}_0 - \tilde{M} = (M_0^A - M^A) + (M_0^B - M^B) + (M^A + M^B - \tilde{M}). \tag{40}$$

According to our assumption, the first two terms on the right-hand side are positive. Because of the loss of energy by gravitational radiation the last term has to be positive, too,

$$\tilde{M} < M^A + M^B. \tag{41}$$

Hence ($\tilde{M}_0 > 0$) the relative binding energy of the resulting body is positive,

$$\tilde{E}_b = 1 - \frac{\tilde{M}}{\tilde{M}_0} > 0. \tag{42}$$

Applying this result to our disks of dust we may exclude the "strange" branch (Fig. 3, $b > 4.1074\ldots$) of the RCR disk solution: RCR disks with $b > 4.1074\ldots$, $E_b < 0$ cannot form by collisions.

From now on, we confine ourselves to colliding RR disks with *equal* baryonic masses, $M_0^A = M_0^B = M_0$. Then, Eq. (39) takes the form

$$\tilde{M}_0 = 2M_0. \tag{43}$$

(For dust, the conservation of the baryonic mass is a consequence of the local energy-momentum conservation $T^{ij}{}_{;j} = 0$.)

Because of the existence of an azimuthal killing vector η^i the *angular momentum* is conserved as well. In the first scenario, the two parallel angular momenta J of the two rigidly rotating disks sum up to $2J$ in the final disk,

$$\tilde{J} = 2J. \tag{44}$$

In a second case we will study questions connected with the formation of the RCR disk by collisions of two one-component disks with antiparallel angular momenta as described in Sec. II A 1 and assume the conservation of the angular momentum for each component separately,

$$\pm\tilde{J} = \pm J \tag{45}$$

(the resulting angular momentum of the initial RR disks and the final RCR disk vanishes). It should be emphasized that the assumption (45) is not very realistic. A small amount of friction between the two dust components would violate the separate conservation of the angular momenta. Nevertheless an assumption like (45) can lead to deeper insight into the physical processes connected with the formation of counterrotating disks and allows, by way of example, a comparison between collisions of disks with parallel and antiparallel angular momenta.

The conservation equations (43)–(45) enable us to calculate the parameters characterizing the final disk as functions of the parameters of the initial RR disks without studying the intermediate, complicated dynamical process.

B. Collision of disks with parallel angular momenta

The equations in Sec. II A 1 show that the combination M_0^2/J of the conserved quantities depends on μ alone (and not on some second parameter). Therefore the relation

$$\frac{\tilde{M}_0^2}{\tilde{J}} \equiv \frac{M_0^2}{J}(\tilde{\mu}) = 2\frac{M_0^2}{J}(\mu) \tag{46}$$

combining the Eqs. (43) and (44) allows us to calculate the parameter $\tilde{\mu}$ of the final disk as a function of μ alone. Using the formulas (B2) and (B3) of appendix B Fig. 5 shows that the initial disk ratio M_0^2/J as a function of μ

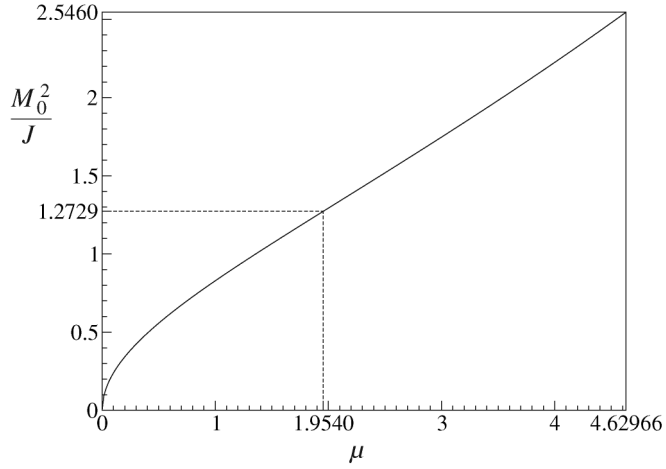

FIG. 5. M_0^2/J of the rigidly rotating disk as function of the centrifugal parameter μ

reaches a maximum of $\max(M_0^2/J) = 2.5460\ldots$ at the ultrarelativistic limit of the disk of dust $\mu = 4.629\,66\ldots$ Thus Eq. (46) cannot have solutions for all values of μ. Obviously, the solutions are restricted to the interval

$$0 \leq \frac{M_0^2}{J} \leq \frac{1}{2}\max\left(\frac{M_0^2}{J}\right) = 1.2729\ldots \tag{47}$$

that is equivalent to the interval

$$0 \leq \mu \leq 1.9540\ldots, \tag{48}$$

cf. the first picture of Fig. 7.

Only for initial disks in this parameter range can the collision again lead to a rigidly rotating disk of dust. Beyond the limit $\mu = 1.9540\ldots$ a collision must lead to other final states, e.g. black holes or black holes surrounded by matter rings.

On the other hand, $\tilde{\mu}$ can take on all values in the interval $[0, 4.629\,66\ldots]$ being considered, i.e. there is no restriction on the parameters of the resulting RR disks. That means *every rigidly rotating disk can be formed in a collision of two rigidly rotating initial disks*. If the centrifugal parameter μ of the initial disks approaches the maximum $\mu = 1.9540\ldots$, then the collision leads to a rigidly rotating disk with $\tilde{\mu} = 4.629\,66\ldots$ arbitrarily close to the extreme Kerr black hole.

Having solved (46) to obtain $\tilde{\mu} = \tilde{\mu}(\mu)$, cf. the first graph of Fig. 7, one may calculate the new coordinate radius $\tilde{\rho}_0$ from (43) via $\tilde{M}(\tilde{\mu}, \tilde{\rho}_0) = 2M_0(\mu, \rho_0)$. The result is plotted in the second graph of Fig. 7.

C. Collision of disks with antiparallel angular momenta

As with the rigidly rotating disk, the ratio M_0^2/J for the counterrotating disk depends only on a centrifugal parameter, here b, and not on ρ_0. With the definition (cf. appendix C)

$$f(\tilde{b}) := \frac{\tilde{M}_0^2}{\tilde{J}} = \frac{[\ln\frac{\sqrt{1+4\tilde{b}^2}}{2}\arctan(2\tilde{b}) - \Im(\mathrm{dilog}\frac{1+2i\tilde{b}}{2})]^2}{\pi[4\tilde{b} - (2 + \ln\frac{\sqrt{1+4\tilde{b}^2}}{2})\arctan(2\tilde{b}) + \Im(\mathrm{dilog}\frac{1+2i\tilde{b}}{2})]} \tag{49}$$

and with the conservation equations (43) and (45) one finds

$$\frac{\tilde{M}_0^2}{\tilde{J}}(\tilde{b}) \equiv f(\tilde{b}) = 4\frac{M_0^2}{J}(\mu), \tag{50}$$

which can be used to calculate the counterrotating disk parameter $\tilde{b}$ as a function of the initial disk parameter μ.

Similar to the case of scenario (a), by using the formulas of the appendices B and C it turns out, that (50) does not have solutions $\tilde{b}$ for all values μ in the allowed range $0 \leq \mu \leq 4.629\,66\ldots$ Fig. 6 shows that $f(\tilde{b})$ reaches a maximum of $f_{\max} = 0.963\,44\ldots$ for $\tilde{b} = b_{\max} = 1.339\,34\ldots$, while the right hand side of (50) grows to much larger values. Thus the formation of a counterrotating disk is only possible in the small range

$$0 \leq \frac{M_0^2}{J} \leq \frac{1}{4}f_{\max} = 0.2408\ldots, \tag{51}$$

i.e. from initial disks in the parameter range

$$0 \leq \mu \leq 0.101\,003\ldots. \tag{52}$$

For values of μ in this interval Eq. (50) always has two solutions: $\tilde{b}$ can be smaller or larger than $b_{\max}$, $\tilde{b} \lessgtr b_{\max}$. Later it will turn out, that in general only the solution $\tilde{b} < b_{\max}$ is of physical relevance, since the formation of a counterrotating disk system with the larger value of $\tilde{b}$ would only be possible if external energy were put into the system.

Finally, if $\tilde{b}$ has been calculated, (43) can be used to determine $\tilde{\rho}_0$.

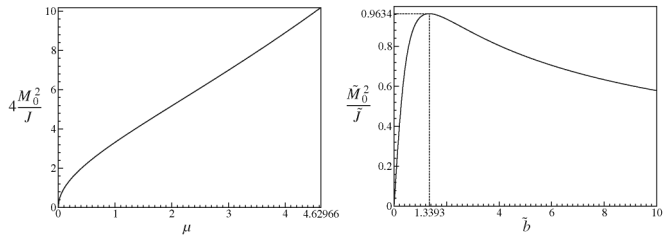

FIG. 6. Baryonic mass M_0 and angular momentum J before and after the collision, cf. Eq. (50).

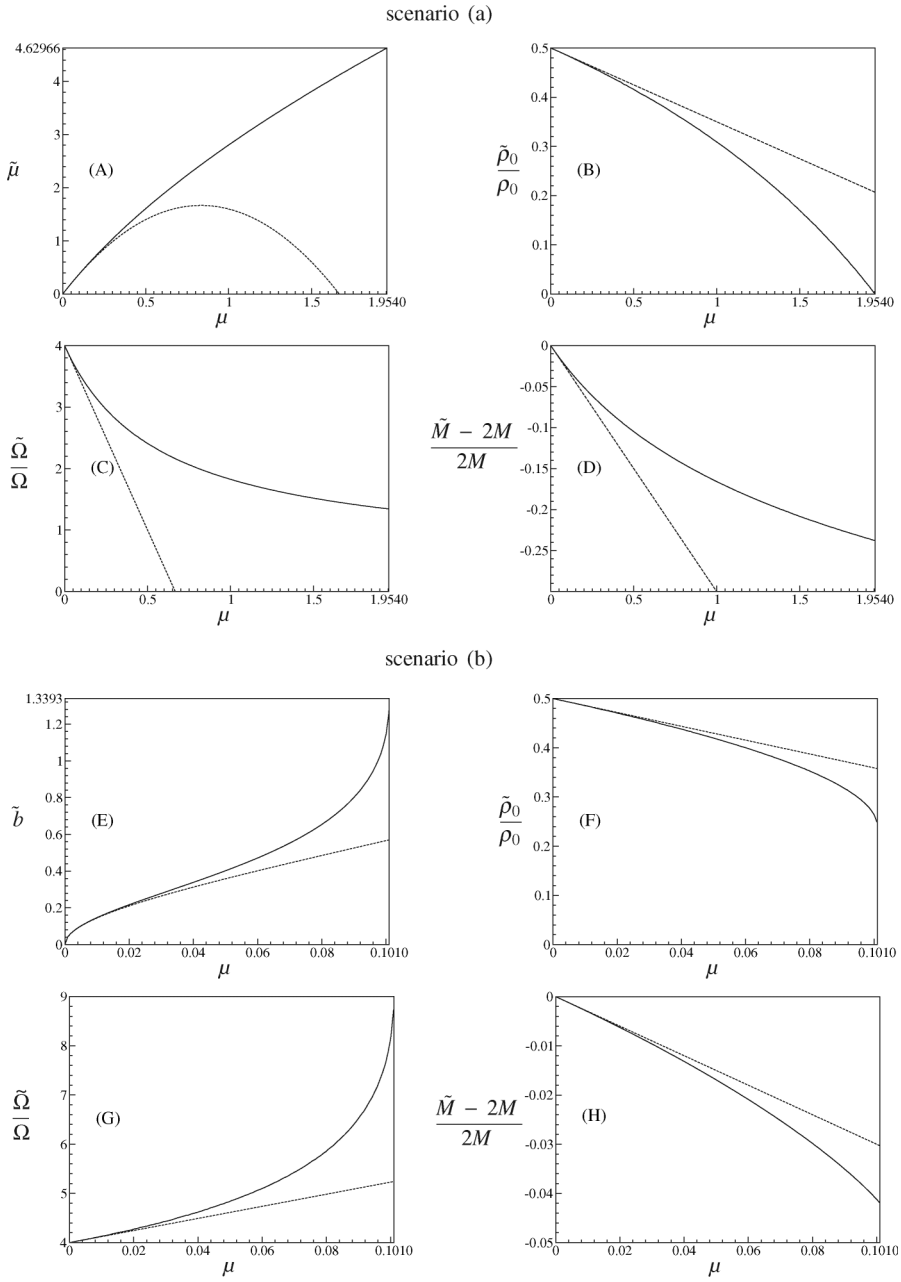

FIG. 7. Parameters of the resulting disks after collision (tilded quantities) as functions of the initial disk parameter μ in the allowed range $0 \leq \mu \leq 1.9540\ldots$ [scenario (a)] and $0 \leq \mu \leq 0.101\,003\ldots$ [scenario (b)] compared with the post-Newtonian approximations for small μ (dashed lines), cf. Sec. IV B. μ, Ω, ρ_0 and M belong to the initial disks.

IV. PROPERTIES OF THE MERGED DISKS

A. General parameter conditions

In the last section we showed which initial parameters can lead to rigidly rotating or counterrotating disks after a collision. Now we will discuss the parameters of the resulting disks as functions of the initial parameters. For this purpose we make use of the explicit expressions for mass M, baryonic mass M_0 and angular momentum J, (B1)–(B3), (C6), and (C8), and plug them into the conservation laws (43), (46), and (50). In this way we obtain the desired parameter relations implicitly in terms of elliptic functions. In Fig. 7 one can see a number of parameter relations generated by a numerical evaluation of those implicit relations (solid lines). They may be compared with the corresponding post-Newtonian approximations derived in subsection IV B (dotted lines). As expected, the curves agree well for small values of the centrifugal parameter μ, but differ for larger μ even qualitatively.

As mentioned earlier [Eq. (48)], in scenario (a) the formation of an RR disk after the collision is only possible for $0 \leq \mu \leq 1.9540\ldots$ while for the final disk all parame-

ters $0 \leq \tilde{\mu} \leq 4.62966\ldots$ are allowed [Fig. 7(a)]. The new coordinate radius $\tilde{\rho}_0$ is one half of ρ_0 in the Newtonian limit, but smaller in the general case. In the limit $\mu = 1.9540\ldots$ the collision leads to a disk in transition to the extreme Kerr black hole with vanishing coordinate radius, $\tilde{\rho}_0 = 0$ [Fig. 7(b)]. The angular velocity increases, maximally by a factor of 4 in the Newtonian limit [Fig. 7(c)]. *For the maximum amount of lost energy $\tilde{M} - 2M$ during the merger process due to gravitational waves one obtains a limit of* 23.8% *of the total initial mass* [Fig. 7(d)].

In scenario (b) the formation of an RCR disk is only possible in the small parameter range $0 \leq \mu \leq 0.101\,003\ldots$ As mentioned before (Sec. III C), there always exist two values of $\tilde{b}$, $\tilde{b} \leqq b_{\max} = 1.339\,34\ldots$, for a given μ (or M_0^2/J). In the first case ($\tilde{b} < b_{\max}$), the coordinate radius $\tilde{\rho}_0$ shrinks to one half of the initial radius or smaller, but never reaches zero [Fig. 7(f)]. The angular velocity increases by a factor of 4 or larger [Fig. 7(g)] and *the limit for the relative energy loss is* 4.2% [Fig. 7(h)]. In the second case ($\tilde{b} > b_{\max}$), the new coordinate radius $\tilde{\rho}_0$ is arbitrarily small for small μ [Fig. 8(b)] and the angular velocity grows to infinity for $\mu \to 0$ [Fig. 8(c)].

We have seen that the emission condition (41)

$$\tilde{M} < M^A + M^B = 2M \tag{53}$$

forbids the formation of RCR disks with negative binding energy ($\tilde{b} > 4.1074\ldots$). The preceding analysis together with the exclusion of energy transfer into the system (53) *enlarges* the forbidden $\tilde{b}$-interval and *restricts* the formation of RCR disks aditionally. Figures 7(h) and 8(d) show that Eq. (53) is completely satisfied for the first interval ($0 < \tilde{b} \leq b_{\max} = 1.339\,34\ldots$) and holds for the small piece $0.0728\ldots \leq \mu \leq 0.101\,003\ldots$ of the second interval corresponding to $1.339\,34\ldots \leq \tilde{b} \leq 3.8038\ldots$ but is violated for $0 \leq \mu < 0.0728\ldots$ which corresponds to $3.8038\ldots < \tilde{b} < \infty$. Obviously, this implies our former result that RCR disks formed by collisions have always a positive binding energy, $\tilde{E}_b > 0$ for $\tilde{b} < 4.1074\ldots$

Adding now the result of Sec. II B where we showed the instability of RCR disks in the interval $b > 1.3393\ldots$ we conclude that for physical reasons *we cannot expect the formation of RCR disks in the second branch* $b > 1.3393\ldots$

B. Analytic parameter conditions for weakly relativistic disks

For most astrophysical applications, rigidly rotating disk models are characterized by very small values of the centrifugal parameter, $\mu \ll 1$. For such weakly relativistic disks it is useful and possible to obtain analytic parameter conditions derived by post-Newtonian expansions of the equations of state and the conservation laws (46) and (50). [For counterrotating disks, for which Eq. (50) has two solution branches, we restrict ourselves to solutions with $\tilde{b} \ll b_{\max}$ excluding the "strange" branch with negative binding energy.]

1. Scenario (a)

The expansion of the relations in appendix B in a power series for μ leads to

$$\Omega M = \frac{\sqrt{2}}{\pi}\left(\frac{1}{3}\mu^{3/2} - \frac{1}{10}\mu^{5/2}\right) + \mathcal{O}(\mu^{7/2}), \tag{54}$$

$$\Omega M_0 = \frac{\sqrt{2}}{3\pi}\left(\mu^{3/2} - \frac{1}{5}\mu^{5/2}\right) + \mathcal{O}(\mu^{7/2}), \tag{55}$$

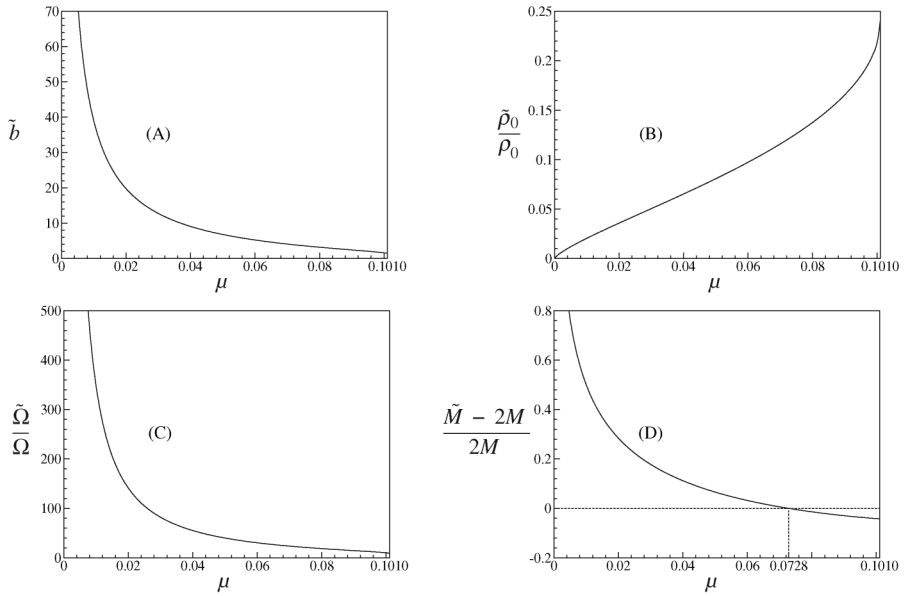

FIG. 8. Behavior of the parameters of the resulting RCR disks [scenario (b)] for the solutions $\tilde{b} > b_{\max}$.

and

$$\Omega^2 J = \frac{\sqrt{2}}{15\pi}\left(\mu^{5/2} - \frac{1}{2}\mu^{7/2}\right) + \mathcal{O}(\mu^{9/2}). \quad (56)$$

The conservation equation (46) now can be written as

$$10\tilde{\mu}^{1/2} + \tilde{\mu}^{3/2} + \mathcal{O}(\tilde{\mu}^{5/2}) = 2(10\mu^{1/2} + \mu^{3/2}) + \mathcal{O}(\mu^{5/2}) \quad (57)$$

with the solution

$$\tilde{\mu} = 4\mu - \tfrac{12}{5}\mu^2 + \mathcal{O}(\mu^3). \quad (58)$$

With $\tilde{\mu}$ and the expansions (55) and $\omega = \Omega\rho_0 = 1/\sqrt{2}(\mu^{1/2} - 1/2\mu^{3/2}) + \mathcal{O}(\mu^{5/2})$ one can calculate $\tilde{\rho}_0$ from Eq. (43),

$$\tilde{\rho}_0/\rho_0 = \tfrac{1}{2} - \tfrac{3}{20}\mu + \mathcal{O}(\mu^2). \quad (59)$$

That means, in the lowest order, the new coordinate radius is one half of the original radius. For the change of the angular velocity, we obtain

$$\tilde{\Omega}/\Omega = 4 - 6\mu + \mathcal{O}(\mu^2), \quad (60)$$

i.e. the rotation of the final disk will be 4 times faster than the rotation of the initial disks in the lowest order. By comparing the gravitational masses of the two initial disks and the final disk, one can determine the energy loss due to gravitational radiation during the dynamical process. The relative energy loss is

$$(\tilde{M} - 2M)/2M = -\tfrac{3}{10}\mu + \mathcal{O}(\mu^2), \quad (61)$$

where the minus sign shows, that the energy indeed leaves the system.

To compare the post-Newtonian approximations with the exact parameter conditions of the last section they are plotted in Fig. 7 as dotted curves.

2. Scenario (b)

With the expansion of Eq. (49) in terms of the centrifugal parameter $\tilde{b}$, $f(\tilde{b}) = \frac{4}{3\pi}(5\tilde{b} - \frac{64}{7}\tilde{b}^3) + \mathcal{O}(\tilde{b}^5)$, Eq. (50) takes the form

$$(10\mu^{1/2} + \mu^{3/2}) + \mathcal{O}(\mu^{5/2}) = \sqrt{2}\left(5\tilde{b} - \frac{64}{7}\tilde{b}^3\right) + \mathcal{O}(\tilde{b}^5) \quad (62)$$

with the solution

$$\tilde{b} = \sqrt{2}\left(\mu^{1/2} + \frac{263}{70}\mu^{3/2}\right) + \mathcal{O}(\mu^{5/2}). \quad (63)$$

From this and with $\tilde{M}_0 = 4\tilde{\rho}_0/3\pi(\tilde{b}^2 - \frac{11}{5}\tilde{b}^4 + \mathcal{O}(\tilde{b}^6))$ one finds for the coordinate radius of the disk

$$\tilde{\rho}_0/\rho_0 = \tfrac{1}{2} - \tfrac{197}{140}\mu + \mathcal{O}(\mu^2). \quad (64)$$

The change of the angular velocity can be calculated from $\Omega = \omega/\rho_0$ and $\tilde{\Omega} = \tilde{b}/(\tilde{\rho}_0\sqrt{1 + 4\tilde{b}^2})$. It leads to

$$\tilde{\Omega}/\Omega = 4 + \tfrac{86}{7}\mu + \mathcal{O}(\mu^2). \quad (65)$$

For the relative energy loss one obtains

$$(\tilde{M} - 2M)/2M = -\tfrac{3}{10}\mu + \mathcal{O}(\mu^2). \quad (66)$$

Comparing the collisions of disks with parallel and antiparallel angular momenta, it turns out, that to the lowest order, the change of the angular velocity and the change of the coordinate radius are equal in both scenarios. Namely, the lowest order terms represent the Newtonian results and in the Newtonian theory there is no influence of the direction of rotation on the gravitational field. Interestingly, a similar effect occurs in the post-Newtonian regime: The energy loss for both scenarios also coincides to the lowest order.

As an example, one can calculate the energy loss for the merger of two disks with mass and radius of our milky way ($\rho_0 = 15\,000$ pc and $M = 2 \times 10^{11} M_\odot$, respectively). The corresponding centrifugal parameter $\mu = 3 \times 10^{-6}$ is so small that the post-Newtonian approximation is sufficient to calculate the efficiency. With Eq. (66) one finds for the energy loss $\Delta M = \tilde{M} - 2M = -4 \times 10^5 M_\odot$ for both scenarios.

V. THE EFFICIENCY OF GRAVITATIONAL EMISSION

An important quantity in the collision process is its efficiency η, which is the negative value of the relative energy loss,

$$\eta = \frac{2M - \tilde{M}}{2M}. \quad (67)$$

Obviously, η is the *upper limit* for the energy transported away by gravitational radiation. (Some part of the energy will also dissipate due to friction. To guarantee the formation of a new rigidly rotating or rigidly counterrotating disk, friction is necessary to force a constant angular velocity.)

As shown in Sec. IV B, for weakly relativistic disks the efficiency is given as

$$\eta \approx 0.3\mu, \quad (68)$$

cf. (61).

In Sec. IV A we already presented the relative energy loss as a function of the centrifugal parameter μ of the initial disks, cf. Fig. 7(d). Here we derive a more explicit expression for the efficiency making use of the scaling behavior of the disks: M/M_0 and M_0^2/J are functions of the centrifugal parameter alone (μ for RR and b for RCR). Therefore M/M_0 is a function of M_0^2/J,

$$\frac{M}{M_0} = F(x), \qquad x := \frac{M_0^2}{J}. \quad (69)$$

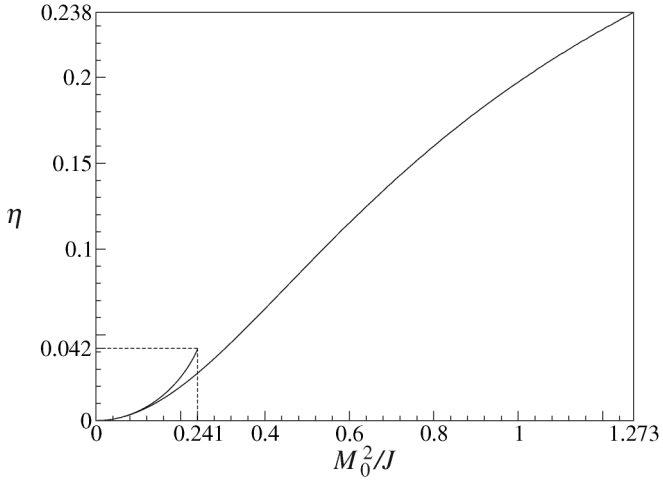

FIG. 9. The efficiency η for scenario (a) (long curve) and scenario (b) (short curve) as function of the physical quantity M_0^2/J of the initial RR disks up to the natural end points of the intervals for which disk formation is possible.

Using the conservation laws (43) and (44) or (45) we obtain the following expressions for the efficiency η as a function of the quantity M_0^2/J of the initial disks,

$$\eta(x) = 1 - \frac{F(2x)}{F(x)} \qquad \text{for scenario (a)}, \tag{70}$$

$$\eta(x) = 1 - \frac{\tilde{F}(4x)}{F(x)} \qquad \text{for scenario (b)}, \tag{71}$$

where F and $\tilde{F}$ can be calculated in terms of elliptic functions from the equations of state of the RR disks and the RCR disks, respectively. Accordingly, η is determined completely by the relative binding energy $E_b = 1 - M/M_0 = 1 - F(x)$ of the RR or RCR disks.

The efficiencies (70) and (71) are plotted in Fig. 9. Note that the efficiency measures the energy *loss*. The picture shows that the formation of a counterrotating RCR disk [scenario (b)] is ''more efficient'' than the formation of a rigidly rotating disk [scenario (a)] for initial disks with the same amount of angular momentum and baryonic mass, but is possible only in a much smaller parameter range. It ends with a comparably small maximum value of $\eta \approx 4.2\%$. The limit $\eta \approx 23.8\%$ for the collision of disks with parallel angular momenta has the order of magnitude of Hawking's and Ellis' limit $\eta \approx 29.3\%$ for the coalescence of two spherically symmetric black holes.

VI. CONCLUSION

In this paper we have discussed the collision and merger processes of rigidly rotating (RR) disks leading again to a RR disk or a rigidly counterrotating (RCR) disk. The conservation equations for mass and angular momentum showed, that these processes are restricted to limited parameter intervals for the initial disks: Only for rigidly rotating disks whose centrifugal parameter μ does not exceed a given maximum value do these conditions allow the formation of a new rigidly rotating disk, and in an even much smaller parameter range, the process can lead to a counterrotating disk. (But of course, even if the balance equations can be satisfied in these parameter ranges, it is not clear if these processes are dynamically possible.) We were able to calculate the physically relevant relations between the parameters (''equations of state'') by a numerical evaluation of the exact but implicit conditions resulting from the conservation equations. Explicit analytical expressions could be derived for the post-Newtonian domain.

It turned out, that every RR disk can be the result of such a collision process (every point of the two-dimensional parameter range can be reached), while the formation of RCR disks is restricted. RCR disks with negative binding energy (as described by a branch of the RCR solution) cannot be formed in a collision process. An interesting result is the calculated upper limit for the efficiency of $\eta \approx 23.8\%$ for the formation of RR disks and of $\eta \approx 4.2\%$ for the formation of RCR disks.

Counterrotating disks are interesting initial configurations for axisymmetric collapse scenarios with gravitational emission. In these cases, the mathematical analysis consists in the discussion of initial-boundary problems for the vacuum Einstein equations. A typical example will be published elsewhere.

ACKNOWLEDGMENTS

We would like to thank David Petroff for many valuable discussions. This work was funded by SFB/Transregio 7 ''Gravitationswellenastronomie''.

APPENDIX A: WHY RIGID ROTATION?

If there is a small amount of friction between the dust rings (which can be anticipated for every realistic system), differentially rotating disks will develop towards an equilibrium state with rigid rotation. Because of the loss of energy via gravitational or thermal radiation the gravitational mass M of the disk decreases in these processes. Therefore we expect to find rigidly rotating disks as minima of the gravitational mass M compared to differentially rotating disks with the same baryonic mass M_0 and the same angular momentum J. Here, we show that M indeed takes an extremum.[1]

[1]To avoid confusion we want to point out that we use two different kinds of variational principles in this paper. In this section, we compare different *solutions* to the Einstein equations (with different rotational laws) to find the rigidly rotating disks as extrema of the gravitational mass M. In contrast to this we consider *trial functions* that do *not* solve the field equations in Sec. II B to find the solutions as extrema of the thermodynamic potential E.

Following the calculations in [12], one can generalize the Gibbs formula (15) to disks with differential rotation $\Omega = \Omega(\rho)$. The result is

$$\delta M = \int_{t=t_0} [\mu_0 \delta(\rho_{M_0}\sqrt{-g}) + \Omega\delta(\rho_J\sqrt{-g})]\mathrm{d}^3x, \quad \text{(A1)}$$

where $\mu_0 = \mu_0(\rho)$ is the chemical potential (specific free enthalpy), g is the determinant of the metric tensor and ρ_{M_0} and ρ_J denote the densities of baryonic mass and angular momentum, respectively, defined by

$$M_0 = \int_{t=t_0} \rho_{M_0}\sqrt{-g}\mathrm{d}^3x, \qquad J = \int_{t=t_0} \rho_J\sqrt{-g}\mathrm{d}^3x. \quad \text{(A2)}$$

If one now considers the set of all disks with different rotation laws $\Omega = \Omega(\rho)$, but fixed baryonic mass and angular momentum, i.e. with the constraints

$$C_1 := M_0 = \text{constant}, \qquad C_2 := J = \text{constant}, \quad \text{(A3)}$$

then one can find the disks with extremal gravitational mass M (and accordingly—due to $M_0 =$ constant—with extremal binding energy $M_0 - M$). With the Lagrange multipliers λ_1 and λ_2, the condition for a stationary point is

$$\delta(M + \lambda_1 C_1 + \lambda_2 C_2) = 0. \quad \text{(A4)}$$

Using (A1)–(A3), the latter equation takes the form

$$\int_{t=t_0} [(\mu_0 + \lambda_1)\delta(\rho_{M_0}\sqrt{-g}) + (\Omega + \lambda_2)\delta(\rho_J\sqrt{-g})]\mathrm{d}^3x = 0. \quad \text{(A5)}$$

Since ρ_{M_0} and ρ_J are varied independently, one finds

$$\Omega = \text{constant}, \qquad \mu_0 = \text{constant}, \quad \text{(A6)}$$

i.e. the family of rigidly rotating disks of dust.

The same considerations are valid for counterrotating disks of dust. The generalization of Eq. (A1) is

$$\delta M = \sum_{i=1}^{2} \int_{t=t_0} [\overset{(i)}{\mu}_0 \delta(\overset{(i)}{\rho}_{M_0}\sqrt{-g}) + \overset{(i)}{\Omega}\delta(\overset{(i)}{\rho}_J\sqrt{-g})]\mathrm{d}^3x, \quad \text{(A7)}$$

where the index i distinguishes between the two fluid components. With the restriction to disks with the same chemical potential ($\overset{(1)}{\mu}_0 = \overset{(2)}{\mu}_0 =: \frac{1}{2}\mu_0$) and baryonic mass density ($\overset{(1)}{\rho}_{M_0} = \overset{(2)}{\rho}_{M_0} =: \frac{1}{2}\rho_{M_0}$) and opposite values of angular velocity ($\overset{(1)}{\Omega} = -\overset{(2)}{\Omega} =: \Omega$) and angular momentum density ($\overset{(1)}{\rho}_J = -(2)\rho_J =: \rho_J$), Eq. (A7) reduces to Eq. (A1), i.e. the extremal problem leads to the *rigidly* counterrotating disks with $\Omega =$ constant.

APPENDIX B: MULTIPOLE MOMENTS OF THE RIGIDLY ROTATING DISK

By specifying the formulas of the general solution to the axis of symmetry, it is possible to calculate all multipole moments of the disk [16]. In particular, one can derive expressions for the gravitational (ADM) mass M, the baryonic mass M_0 and the angular momentum J,

$$\Omega M(\mu) = -\tfrac{1}{2}(\omega(\mu)a_1(\mu) + b_0(\mu)), \quad \text{(B1)}$$

$$\Omega M_0(\mu) = \frac{\sqrt{2\mu}}{4}a_1(\mu), \quad \text{(B2)}$$

$$\Omega^2 J(\mu) = -\tfrac{1}{2}(\omega(\mu)a_1(\mu) + \tfrac{1}{2}b_0(\mu)), \quad \text{(B3)}$$

where one needs the relations

$$a_1 = \frac{1}{\sqrt{\mu}}\left[2\sqrt{1+\mu^2}I_0(\mu)\left(h'^2 - \frac{E(h)}{K(h)}\right) + I_1(\mu) + (1+\mu^2)^{1/4}\frac{\pi}{K(h)}\Lambda_0(\mathrm{am}(\hat{I}(\mu), h'), h))\right]$$

$$\equiv \frac{1}{\sqrt{\mu}}\left[\sqrt{\frac{2}{hh'}}(E[\mathrm{am}(\hat{I}(\mu), h'), h'] - h^2\hat{I}) + I_1(\mu)\right],$$

$$b_0 = -\frac{1}{h(\mu)}\mathrm{sn}(\hat{I}(\mu), h'(\mu))\mathrm{dn}(\hat{I}(\mu), h'(\mu)),$$

$$\omega = \Omega\rho_0 = \frac{1}{2}\sqrt{1 - \frac{h'^2(\mu)}{h^2(\mu)}}\mathrm{cn}(\hat{I}(\mu), h'(\mu)),$$

$$\mathrm{e}^{2V_0} = \frac{h'(\mu)}{h(\mu)}\mathrm{cn}^2(\hat{I}(\mu), h'(\mu)),$$

$$h = \sqrt{\frac{1}{2}\left(1 + \frac{\mu}{\sqrt{1+\mu^2}}\right)}, \qquad h' = \sqrt{1-h^2},$$

$$I_n = \frac{1}{\pi}\int_0^\mu \frac{\ln(\sqrt{1+x^2}+x)}{\sqrt{1+x^2}}\frac{x^n}{\sqrt{\mu - x}}\mathrm{d}x,$$

$$\hat{I} = (1+\mu^2)^{1/4}I_0(\mu),$$

with the complete elliptic integrals $K(k) = F(\pi/2, k)$ and $E(k) = E(\pi/2, k)$, Heumann's Lambda function $\Lambda_0(\psi, k) = \frac{2}{\pi}[E(k)F(\psi, k') + K(k)E(\psi, k') - K(k)F(\psi, k')]$, $k' = \sqrt{1-k^2}$ and the Jacobian elliptic functions sn, cn, dn and am.

APPENDIX C: MULTIPOLE MOMENTS OF THE RIGIDLY COUNTERROTATING DISK

For the metric (9), by using the field equations, the relations (6)–(8) for mass and angular momentum can be expressed using only the metric potential U and its ρ- and ζ-derivative in the disk. For general counterrotating disks one finds

$$M = \int_0^{\rho_0} U_{,\zeta}\rho\mathrm{d}\rho, \quad \text{(C1)}$$

$$M_0 = \int_0^{\rho_0} \mathrm{e}^{-U}\sqrt{(1-2\rho U_{,\rho})(1-\rho U_{,\rho})}U_{,\zeta}\rho \mathrm{d}\rho \quad \text{(C2)}$$

and

$$J = \frac{1}{2}\int_0^{\rho_0} \mathrm{e}^{-2U}\sqrt{\rho U_{,\rho}(1-\rho U_{,\rho})}U_{,\zeta}\rho^2 \mathrm{d}\rho. \quad \text{(C3)}$$

These equations can be applied to rigidly counterrotating disks (RCR disks) with the explicit expressions (see [6])

$$U(\rho, \zeta = 0) = \frac{1}{2}\ln\left[\frac{\Omega\rho_0}{2b}(1+\sqrt{1+4b^2\rho^2/\rho_0^2})\right], \quad \text{(C4)}$$

$$U_{,\zeta}(\rho, \zeta = 0+) = \frac{2b}{\pi\rho_0}\frac{1}{\sqrt{1+4b^2\rho^2/\rho_0^2}}\arctan\frac{2b\sqrt{1-\rho^2/\rho_0^2}}{\sqrt{1+4b^2\rho^2/\rho_0^2}}, \quad \text{(C5)}$$

where $\Omega = b/(\rho_0\sqrt{1+4b^2})$ is the constant angular velocity. They lead to

$$M = \frac{\rho_0}{\pi}\left(1-\frac{1}{2b}\arctan(2b)\right), \quad \text{(C6)}$$

$$M_0 = \frac{\rho_0}{4\pi b}(1+4b^2)^{1/4}\left[\ln\frac{\sqrt{1+4b^2}}{2}\arctan(2b) - \Im\left(\mathrm{dilog}\frac{1+2\mathrm{i}b}{2}\right)\right] \quad \text{(C7)}$$

and

$$J = \frac{\rho_0^2}{16\pi b^2}\sqrt{1+4b^2}\left[4b - \left(2+\ln\frac{\sqrt{1+4b^2}}{2}\right)\arctan(2b) + \Im\left(\mathrm{dilog}\frac{1+2\mathrm{i}b}{2}\right)\right] \quad \text{(C8)}$$

with the dilogarithm function

$$\mathrm{dilog}\,(z) = \int_1^z \frac{\ln w}{1-w}\mathrm{d}w. \quad \text{(C9)}$$

APPENDIX D: THE COUNTERROTATING DISK OF DUST METRIC

The inverse scattering method (cf. [17]) can be used to calculate the function $U(\rho, \zeta)$ in the line element (9) of the counterrotating RCR disk. For an angular velocity Ω and a coordinate radius ρ_0 it leads to

$$U(\rho,\zeta) = \frac{1}{4\pi}\int_{-1}^{1}\frac{\ln[1-\alpha(1-k^2)]}{\sqrt{(\mathrm{i}k-\zeta/\rho_0)^2+\rho^2/\rho_0^2}}\mathrm{d}k, \qquad \alpha := 4\Omega^2\rho_0^2. \quad \text{(D1)}$$

By using elliptical coordinates (ξ, η) with

$$\rho = \rho_0\sqrt{(1+\xi^2)(1-\eta^2)}, \qquad \zeta = \rho_0\xi\eta, \quad \text{(D2)}$$

it is possible to express U in terms of the dilogarithm function (C9). The result is

$$U = \frac{1}{2\pi}\arctan\frac{1}{\xi}\cdot\ln\left[\frac{\alpha}{4}(1+\xi^2)(1+\eta)^2\right] - \frac{1}{2}\mathrm{Artanh}\,\eta - \frac{1}{2}\ln n - \frac{1}{2\pi}\Im\sum_{j=1}^{2}[\mathrm{dilog}A_j^+ + \mathrm{dilog}A_j^-], \quad \text{(D3)}$$

where

$$A_j^{\pm} = 1 - \frac{\beta(1-\eta)(\xi+\mathrm{i})}{(-1)^j\sqrt{1+\beta^2(1+\xi^2-\eta^2)\pm 2\beta\xi\eta}-(\beta\xi\eta\pm 1)}, \qquad \beta := \sqrt{\frac{\alpha}{1-\alpha}} \quad \text{(D4)}$$

and

$$n = \frac{\sqrt{1+\beta^2(1+\xi^2-\eta^2)+2\beta\xi\eta}-1-\beta\xi\eta}{\beta\sqrt{(1+\xi^2)(1-\eta^2)}}. \quad \text{(D5)}$$

The function k can be calculated from U via line integration by using the field equations

$$k_{,\rho} = \rho(U_{,\rho}^2 - U_{,\zeta}^2), \qquad k_{,\zeta} = 2\rho U_{,\rho}U_{,\zeta}. \quad \text{(D6)}$$

[1] G. Neugebauer and R. Meinel, Astrophys. J. **414**, L97 (1993).
[2] G. Neugebauer and R. Meinel, Phys. Rev. Lett. **73**, 2166 (1994).
[3] G. Neugebauer and R. Meinel, Phys. Rev. Lett. **75**, 3046 (1995).
[4] J. M. Bardeen and R. V. Wagoner, Astrophys. J. **158**, L65 (1969).
[5] J. M. Bardeen and R. V. Wagoner, Astrophys. J. **167**, 359 (1971).
[6] T. Morgan and L. Morgan, Phys. Rev. **183**, 1097 (1969); **188**, 2544(E) (1969).
[7] J. Bičák, D. Lynden-Bell, and J. Katz, Phys. Rev. D **47**, 4334 (1993).
[8] W. Meinhardt, Ph.D. thesis, Friedrich-Schiller-Universität Jena, 1994.
[9] S. W. Hawking and G. F. R. Ellis, *The Large Scale Structure of Space-Time (Cambridge Monographs on Mathematical Physics)* (Cambridge University Press, Cambridge, England, 1973).
[10] G. Neugebauer, A. Kleinwächter, and R. Meinel, Helv. Phys. Acta **69**, 472 (1996).
[11] J. B. Hartle and D. H. Sharp, Astrophys. J. **147**, 317 (1967).
[12] G. Neugebauer, in *Proceedings of the 2nd Hungarian Relativity Workshop, Budapest, 1987*, edited by Z. Perjés (World Scientific, Singapore, 1988), p. 134.
[13] J. Katz, Found. Phys. **33**, 223 (2003).
[14] M. Demiański, *Relativistic Astrophysics (International Series in Natural Philosophy Vol. 110)* (Pergamon Press/ PWN-Polish Scientific Publishers, Oxford/Warsaw, 1993).
[15] G. Neugebauer, Ann. Phys. (Leipzig) **9**, 342 (2000).
[16] A. Kleinwächter, Ann. Phys. (Leipzig) **9**, SI-99 (2000).
[17] G. Neugebauer and R. Meinel, J. Math. Phys. (N.Y.) **44**, 3407 (2003).